Biomaterials Connect
ISSN: 3105-0387
2025, Article ID. 2025.0014, Cite as: https://doi.org/10.69709/BIOMATC.2025.108000

SCIFINITI PUBLISHING

Research Article

OPEN ACCESS

Preparation and Characterization of Biocompatible Hydrogels Based on a Chitosan-Polyacrylamide Copolymer

Elena Rosova[✉,1], Zoolsho Zoolshoev[✉,1] Ekaterina Vyrezkova[✉,2] Elena Vlasova[✉,1] Natalia Smirnova[✉,1] Konstantin Kolbe[✉,1] Natalia Saprykina[✉,1] Ivan Kuryndin[✉,1,*]

[1] Branch of Petersburg Nuclear Physics Institute Named by B.P. Konstantinov of National Research Centre «Kurchatov Institute»—Institute of Macromolecular Compounds, Bolshoy pr., 31, 199004 St. Petersburg, Russia
[2] St. Petersburg State Technological Institute (Technical University), Moskovski pr., 26, 190013 St. Petersburg, Russia

Article History
Received: December 20, 2024 Accepted: March 23, 2025 Published: May 15, 2025

Abstract
Hydrogels comprised of natural and synthetic polymers are widely used in the biomedical field due to their distinguishing properties, such as softness, flexibility, swelling, and biocompatibility. In this study, we obtained and characterized hydrogel materials based on chitosan/acrylamide copolymer as potential matrices for biomedical applications. FTIR studies confirmed the formation of chitosan/polyacrylamide graft copolymer. Kinetics of gel formation was investigated with the rheological tests and the change of reaction mixture viscosity in the shear mode was measured. Scanning electron microscopy revealed a porous surface with micron- and submicron-sized gels. The kinetics of swelling/drying processes in the obtained hydrogels were studied at varying pH values. A significant decrease in the equilibrium swelling degree in an alkaline medium was observed, dropping from 50 g/g in the first cycle to 36 g/g in the second cycle. Mechanical characteristics of the chitosan/polyacrylamide hydrogel-shaped samples were tested both in compression and tension modes. It was found that for the samples swollen at pH 6.8, the tensile and compression strengths were 37 kPa and 19 kPa, respectively. The biological activity of the obtained hydrogels was evaluated by the MTT test. The kinetics of drug release from hydrogels in phosphate buffer was studied using lidocaine hydrochloride as a model compound.

Keywords:
hydrogels; polyacrylamide; chitosan; swelling; biocompatibility

1. Introduction

Currently, a large number of research works are devoted to the development and preparation of new biomaterials with attractive applications in different fields [1–3].

Special attention was paid to swelling hydrogels based on natural and synthetic polymers, which can be used independently as matrices for the formation of composites with various functional and physico-mechanical properties [4–6]. Hydrogel-based materials of specific geometric shapes and purposes are used in cosmetology, biotechnology, tissue engineering, medicine, and pharmaceuticals [7–9]. The presence of a natural component in a hydrogel significantly increases the biocompatibility of these hybrid systems and the possibility of their biomedical application [10–12]. The most common and inexpensive natural polymers are polysaccharides, such as cellulose, chitosan, lignin, collagen, and gelatin [13,14]. Along with the absence of toxicity, they are characterized by biocompatibility, coagulation ability, and the ability to adsorb biopharmaceuticals [15,16]. Among the polymers listed above, chitosan fully meets the requirements for biomaterials used in medicine, cosmetology, and tissue engineering [17–19]. It will be recalled that the preparation of chitosan-based hydrogels (the formation of a crosslinked structure) requires the use of toxic synthetic or expensive natural crosslinkers [20–22]. A pos-

* **Corresponding Author:**
Ivan Kuryndin, Branch of Petersburg Nuclear Physics Institute Named by B.P. Konstantinov of National Research Centre «Kurchatov Institute»—Institute of Macromolecular Compounds, Bolshoy pr., 31, 199004 St. Petersburg, Russia, isk76@mail.ru

© 2025 Copyright by the Authors.
Licensed as an open access article using a CC BY 4.0 license.

sible solution to this problem is to obtain hybrid systems based on synthetic polymers, which enhance mechanical strength by cross-linking macromolecules through transverse covalent bonds and forming a three-dimensional network [23,24]. This approach allows for expanding possible applications of chitosan and other natural polymers.

The choice of a synthetic polymer for the preparation of a hybrid material is limited by the fact that synthesis or processing of these materials is usually carried out in high-temperature melts or solutions in organic solvents, which precludes the possibility of combining them with natural polymers [25]. In this connection, the class of water-soluble synthetic polymers (or polymers synthesized in an aqueous environment) attracts much interest. Among water-soluble monomers, acrylamide deserves special attention because the polymers based on it are biocompatible, hydrophilic, and have good film-forming properties [26–28].

N, N′-Methylene-bis-acrylamide is widely used as a crosslinking agent for synthesizing spatially crosslinked structures of acrylamide. Crosslinked polyacrylamide, due to the presence of hydrophilic groups and a three-dimensional framework, is a hydrogel capable of absorbing large amounts of water, aqueous solutions, and biological fluids [29,30].

Acrylamide is known to form copolymers with hydrophilic and hydrophobic monomers. Graft copolymerization of acrylamide can be used both to modify existing polymers and to obtain new cross-linked hybrid structures [31,32].

Hydrogels based on natural, semi-synthetic, and synthetic polymers are considered innovative materials for biomedical applications. Hydrophilicity, swelling, biocompatibility, mechanical stability, and desired flexibility allow hydrogels to be considered promising drug delivery systems [33]. Compared to other materials such as nanocapsules, micelles, and liposomes, hydrogels exhibit higher drug-loading capacity and provide controlled drug release [34,35].

Hydrogels based on polyacrylamide/chitosan copolymer have been studied sufficiently. At the same time, copolymer hydrogel materials with different functional properties are still of interest to specialists in medical and biotechnological fields including the design of contact lenses, hygiene products, tissue engineering scaffolds, drug delivery systems, and wound dressings [36]. The advantage of these materials lies in their ability to be fabricated into various geometric shapes and sizes during production, depending on the specific application. Additionally, they offer softness, flexibility, and a high degree of transparency [37,38]. The above-mentioned properties make these materials promising for use in ophthalmology [39], and the resulting films with a different thickness and surface area could potentially be used as skin care treatment materials. Mechanical properties are important characteristics of hydrogel materials in their further use for biomedical and cosmetic applications [40]. Improving the mechanical characteristics of hydrogels by modifying the input polymers or introducing fillers often leads to a loss of transparency of the gel or the acquisition of color, whereas for several applications these properties are crucial [41,42].

The aim of this work was to obtain hydrogel materials based on polyacrylamide/chitosan copolymer in the form of cylinders and thin films with appropriate mechanical properties in the swollen state, lack of cytotoxicity and bioactivity, as well as the ability to drug release.

2. Materials and Methods

2.1. Materials

The copolymers based on polyacrylamide (PAA) and chitosan were prepared by graft copolymerization of acrylamide (AA) (SIGMA-ALDRICH, 98%) in solutions of chitosan (LLC «Bioprogress», M_w = 80·10^3 g/mol, DD 90%) in acetic acid (99.8%, Vecton, St. Petersburg, Russia). The polymerization was initiated by ammonium peroxydisulfate (APS) (SIGMA-ALDRICH, 98%) and N, N, N', N'-tetramethylethylenediamine (TEMED) (SIGMA-ALDRICH, 99%) [31].

2.2. Synthesis of Polyacrylamide/Chitosan Hydrogels

Hydrogels were synthesized from acrylamide and chitosan by the addition of a crosslinking agent (N, N'-methylene-bis-acrylamide, MBAA, SIGMA-ALDRICH, 98%) at the grafting stage.

To synthesize hydrogels, 30% aqueous solution of the monomer (AA) was mixed with 1% aqueous solution of the crosslinking agent (MBAA) in the 10:1 ratio (v/v). Then, 1% solution of chitosan in 0.1 M acetic acid (8:2 v/v), TEMED, and APS were added to the reaction mixture [36].

2.3. Rheological Tests

The kinetics of gel formation was investigated using the rheological method by measuring the change in viscosity of the reaction mixture at 25 °C under the shear mode. The measurements were carried out on a "Reotest-2" rotational viscometer (VEB MLW, Germany) with a thermostated cylinder-cylinder working unit (the ratio of cylinder radii was equal to 1.24) at a shear rate of 5.4 s^{-1}.

2025, Vol. 2, Article ID. 2025.0014
https://doi.org/10.69709/BIOMATC.2025.108000

2.4. Obtaining the Samples

To obtain hydrogel samples, the prepared reaction mixture was poured into an appropriate mold, namely, the test tubes, and into the cell with plane-parallel sides with a variable gap. The gelation process was carried out in air at room temperature for 24 h. Then the gel was taken out of the mold and washed in distilled water to remove the residues of acrylamide and the crosslinking agent. Therefore, the samples in the form of cylinders and films were obtained. For further studies, the gels were dried in air to constant weight and then placed in a vacuum drying oven until the moisture was completely removed.

2.5. Morphology and Transparency Tests

The morphology of lyophilized samples was investigated using a SUPRA-55VP scanning electron microscope (ZEISS, Germany). Gel transparency was determined on a UV-vis spectroscopy on an SF-2000 (OKB Spectr, St. Petersburg, Russia) spectrometer. The measurements were carried out at different sections of the sample at least 5 times, and the variation of values did not exceed 2%.

2.6. FTIR Spectra

FTIR spectra of the gel samples were recorded on a Bruker Vertex70 spectrometer using a Pike attenuated total reflectance (ATR) microattachment with a ZnSe working element. During registration of the FTIR spectra, a correction was made that took into account the dependence of penetration depth on wavelength.

2.7. Study of Swelling/Drying Processes

Kinetics of swelling/drying processes in the hydrogels were studied in the media with different pH values: 0.1 M HCl (pH 2.1), distilled water (pH 6.8), and 0.1 M NaOH (pH 12.8). The samples dried in a vacuum to constant weight were placed in the solutions with a given pH at a gel/solution mass ratio of 1/1500 to ensure pH constancy during the swelling process. The weight of the swelling samples was measured at fixed intervals. The swelling degree was calculated according to the Equation (1) [43]:

$$Q = \frac{m - m_0}{m_0} \quad (1)$$

where m is the mass of the swollen sample (g) and m_0 is the mass of the initial dry sample (g).

The swelling process was considered to be completed when the gels reached the equilibrium swelling degree (Q_e), which was characterized by the unchanged weight of a hydrogel during further exposure to the liquid.

Gel drying (liquid desorption) was carried out in air at room temperature until a constant weight was reached; the change in sample mass over time (Δm) was controlled. The mass of the samples was determined gravimetrically with an Analytical balance VL-210 (Gosmetr, St. Petersburg, Russia). Repeated swelling/drying cycles were performed to determine the reversibility of the processes. Each swelling test was performed on at least 3 samples. The spread of swelling/drying degree values was no more than 10%.

2.8. Mechanical Tests

The deformation behavior of hydrogels after their equilibrium swelling was investigated on a 2166 R-5 tensile testing machine (Tochpribor, Ivanovo, Russia). Cylindrical samples and film samples were used for the tests in the uniaxial compression mode at a compression rate of 5 mm/min and in the uniaxial extension mode at a stretching rate of 40 mm/min, respectively. The obtained stress-strain curves were used to determine the values of breaking strength, deformation at break, and elastic modulus [44]. For each sample, the test was performed at least 5 times. The spread of values of mechanical characteristics did not exceed 10% of their values. The Young's modulus (E) corresponded to the elastic modulus under stretching:

$$E = \frac{\sigma}{\varepsilon} \quad (2)$$

where σ is the tensile stress, and ε is the axial strain.

The elastic modulus (G) under compression was calculated according to the following formula:

$$G = \frac{\sigma}{\lambda - \lambda^{-2}} \quad (3)$$

where σ is the stress, λ is the deformation at compression determined as the ratio of the current sample height to the initial sample height.

2.9. Biocompatibility Studies

The biological activity of the obtained hydrogels was evaluated using colorimetric analysis of cell proliferation and cytotoxicity with 3-[4,5-dimethylthiazol-2-yl]-2,5-diphenyltetrazolium bromide (MTT test). The adhesion efficiency, viability, proliferation, and morphology of human dermal fibroblasts during cultivation on the chitosan/PAA hydrogel matrices were assessed. The optical density of the solution was recorded using a SPECTROstar Nano (BMG LABTECH, Ortenberg, Germany). The absorbance of formazan was determined at 570 nm, and the cut-off wavelength was equal to 690 nm.

2.10. Drug Release

Lidocaine hydrochloride (HL) solution was used as a model drug compound to study the release process. For the incorporation of HL into hydrogels, the pre-dried samples were swollen in a 10% aqueous solution of HL to an equilibrium state. The gels were then extracted from the solution, followed by the residual solution removed from the gel surface. Then the swollen hydrogels were used in drug release experiments from hydrogels in a physiological solution (pH 7.4). The concentration of HL was determined by UV-vis spectroscopy at 37 °C and calculated from the calibration dependences of the optical density on the concentration of HL at λ = 264 nm.

3. Results and Discussion

3.1. Investigation of the Gel Formation Process

It has been previously shown that (AA) grafts onto chitosan through its amino and hydroxyl groups. In this work, the formation of graft copolymers was confirmed by FTIR studies [35,36].

The FTIR spectra of PAA, chitosan, and chitosan/PAA copolymer are shown in Figure 1. In the PAA spectrum (1), the bands at 3189 cm^{-1} (valence vibrations of NH_2 group in the primary amide), 1650 cm^{-1} (C=O of the amide group), and 1600 cm^{-1} (deformation vibrations of NH_2 group in the primary amide) are observed. In the FTIR spectrum of chitosan (2) in the salt form, the following characteristic bands can be detected: the wide band at 3500–3100 cm^{-1} (primary and secondary OH groups, protonated NH_3^+ groups, NH of the secondary amide), and the peak at 1647 cm^{-1} (CO group of Amide I). The complex band with a maximum at 1540 cm^{-1} is a superposition of three absorption bands: 1550–1560 cm^{-1} (Amide II), 1560–1530 cm^{-1} (protonated NH_3^+ groups), and 1590–1550 cm^{-1} (COO^- groups of acetate counterions). The presence of acetate counterions is also confirmed by the appearance of the band at 1405 cm^{-1}. The peak at 1150 cm^{-1} is assigned to the valence vibrations of the bridging oxygen; the bands in the 1070–1020 cm^{-1} regions are attributed to C-O vibrations [45,46].

The FTIR spectrum of the chitosan/PAA copolymer contains the bands typical of both PAA and chitosan. However, there are noticeable differences in the 1160–1020 cm^{-1} region of the spectrum that are related to the changes in the glucoside ring of chitosan [47]. To gain a more detailed understanding of the changes occurring in chitosan molecules during copolymer formation, the difference spectrum was obtained by subtracting the PAA spectrum from the chitosan/PAA copolymer spectrum (Figure 2).

When comparing the chitosan spectrum (1) and the difference spectrum (2), the shifts of the following bands: from 1150 cm^{-1} to 1160 cm^{-1}, from 1067 cm^{-1} to 1052 cm^{-1}, and from 1020 cm^{-1} to 1030 cm^{-1} are seen. The variation of the shape of the spectrum in the 1240-1200 cm^{-1} range (Figure 2) may be explained by the appearance of the secondary amino groups (NH) in the copolymer, which agrees with the scheme of formation of copolymer with the participation of the amino groups of chitosan molecule [37].

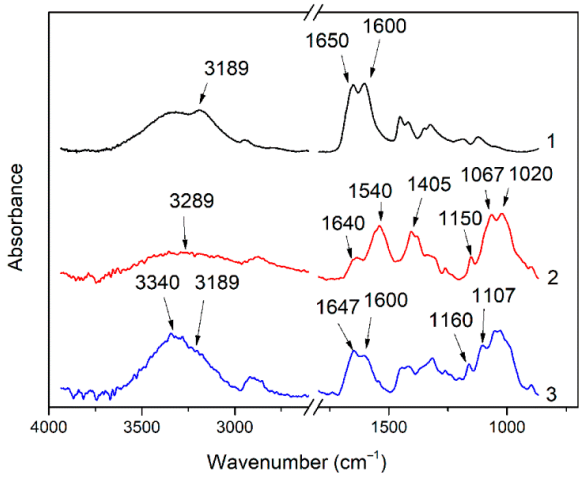


Figure 1: FTIR spectra of PAA (1), chitosan (2), and the chitosan/PAA copolymer (3).

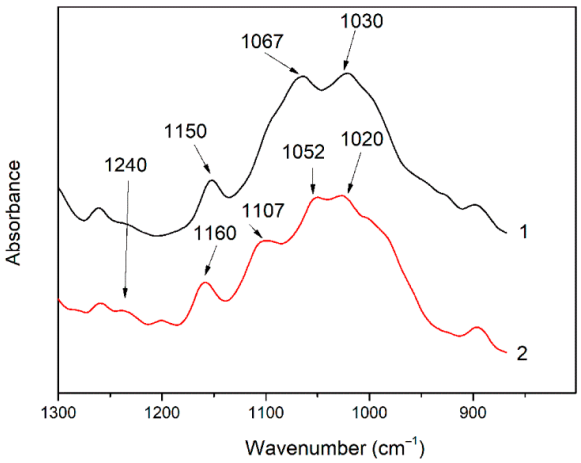


Figure 2: FTIR spectrum of chitosan (1) and the difference spectrum obtained by subtracting the PAA spectrum from the chitosan/PAA copolymer spectrum (2).

The introduction of the crosslinking agent (MBAA) during copolymerization leads to the formation of a crosslinked polymer structure and hydrogel formation [30]. The scheme of the synthesis of the chitosan-acrylamide copolymer and crosslinking of PAA chains with N, N-methylene-bis-acrylamide is presented in Figure 3.

2025, Vol. 2, Article ID. 2025.0014
https://doi.org/10.69709/BIOMATC.2025.108000

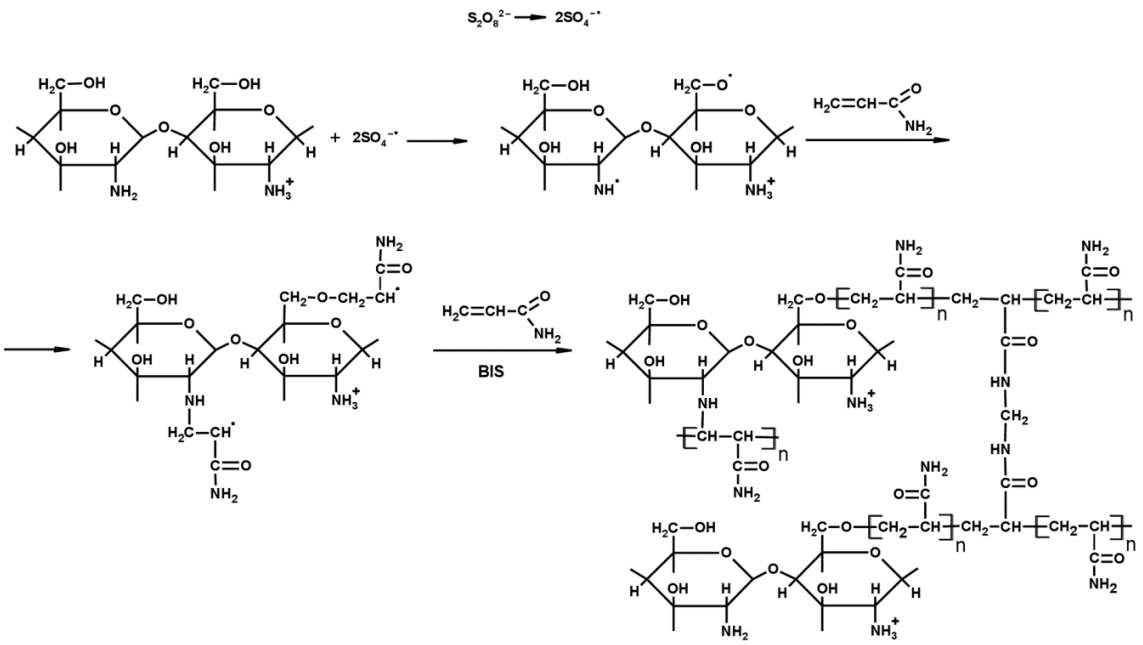


Figure 3: Scheme of formation of the crosslinked chitosan/acrylamide copolymer.

Gels based on cross-linked polymers are incapable of flowing because their macromolecules cannot move relative to each other. At the gelation point, the system loses fluidity, and a sharp increase in the viscosity of the solution is observed. In this work, the gelation time or gel point was determined by the rheological method. The dependence of shear viscosity η on time t was plotted (Figure 4). It can be seen that a sharp increase in the viscosity of the solution, which indicates the onset of gelation, occurs 35 min after the beginning of the experiment.

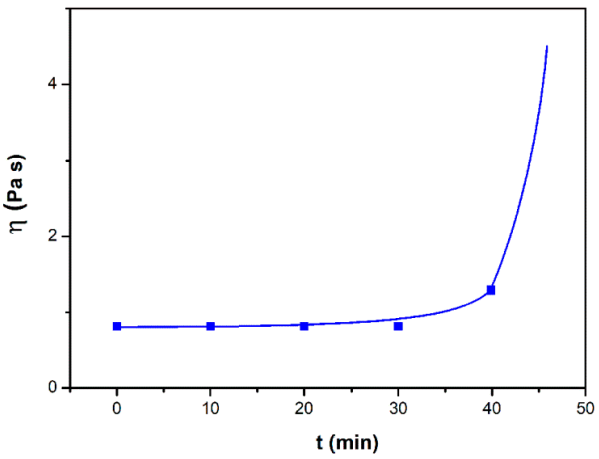


Figure 4: Variation of viscosity of the chitosan/PAA solution with time.

3.2. The Samples Preparation

The obtained hydrogels, both cylinders and films, were colorless, transparent, and homogeneous (Figure 5). The percentage of light transmission was 90–92%. The transparency of the samples did not depend on the film thickness, and the swelling medium did not change during the swelling process. The gap size in the frame during the film production process varied from 0.3 to 2 mm. After removal from the frame, the resulting films had the appropriate thickness, but during the process of swelling in water, the thickness of the films increased twice.

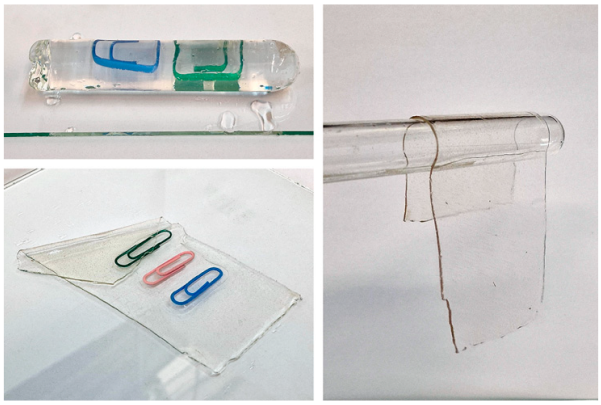


Figure 5: The photographs of different shaped gels.

3.3. Investigation of Swelling/Drying Process

A characteristic property of cross-linked polymer hydrogel structures is their ability to absorb large amounts of a liquid. Such polymers swell strongly in aqueous solutions, absorbing and retaining an amount of liquid well over the dry mass of the polymer. The swelling processes of the obtained chitosan/PAA hydrogels were investigated in a wide pH range of the medium. The hydrogel samples showed the same degree of equilibrium swelling regardless of their shape [48,49].

Figure 6 presents the plots of swelling kinetics of the chitosan/PAA hydrogel samples in aqueous solutions with pH = 2.1 (0.1 M HCl), pH = 6.8 (H_2O dist.), and pH = 12.8 (0.1 M NaOH).

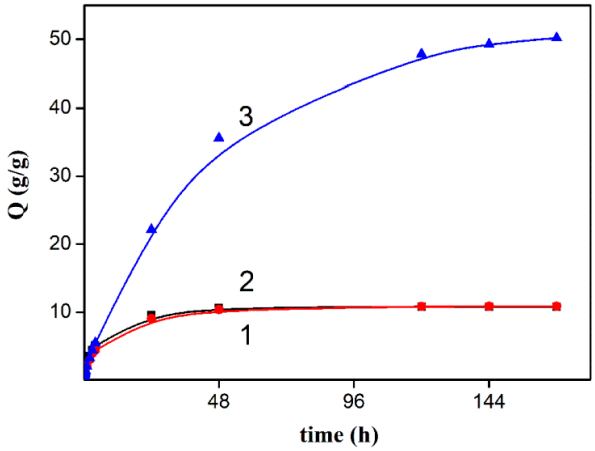


Figure 6: Swelling kinetics of the chitosan/PAA hydrogel samples in aqueous solutions with pH = 2.1 (1), pH = 6.8 (2), and pH = 12.8 (3).

The swelling degree of the samples increases sharply at all pH values during the initial stage, indicating a high rate of solvent diffusion into the gel. It then reaches a plateau, signifying the attainment of equilibrium swelling (Q_e). The time required to reach the Q_e was similar in acidic and neutral media. In an alkaline solution, Q_e was reached for a longer time and achieved a higher value of the equilibrium swelling degree. This is because during swelling in alkali, on the one hand, hydrolysis of PAA and partial conversion of amide groups into carboxylate groups (COO^-) occurs, and on the other hand, chitosan in the hydrogel exists in the salt form and contains acetate groups (CH_3COO^-) in the chain. Upon dissociation of such hydrogel in aqueous solution, the groups carrying charge and counterions are formed. The charged ions in macromolecules are bound to the polymer chains, while counterions remain in the solution in a free state. Due to repulsion between similarly charged units of the spatial network, separation of polymer chains and stretching of the network take place, which eventually results in a high swelling degree [50].

The equilibrium swelling degree of gels in water is much lower than that in alkali. The obtained hydrogel is a weak polyelectrolyte and poorly dissociates into ions in aqueous solution. The polymer network is subjected to a lower deformation degree than that during swelling in alkali, which hinders the diffusion of the solution into the hydrogel.

In an acidic medium, ionization of carboxyl and acetate groups is suppressed due to the presence of excess hydrogen ions; the macromolecule acquires a positive charge, which leads to shielding of charge and weak swelling in an acidic medium.

The hydrogels were dried, and the change in mass of the dried sample after swelling compared to the initial sample was monitored. It was found that the swelling process is completely reversible in acidic and neutral media. The mass of the sample after the swelling-drying cycle was equal to the initial mass. After drying the samples swollen in the alkaline medium, an increase in the sample mass was observed compared to the initial one. An increase in the mass of the dried sample after 3 cycles of swelling-drying was 53%, while the main increase in the mass of the samples occurring after the first cycle was 45%. The observed effect is a result of the interaction of hydrogel components with alkali and salt formation.

The dried samples were subjected to a repeated swelling-drying cycle. It was shown that in the neutral medium, the repetitive swelling process did not differ from the first cycle. In the acidic medium, a slight reduction in the equilibrium swelling degree was observed during the second cycle. The observed effect may be explained by the fact that during the first swelling of the hydrogel in acid, partial acidic hydrolysis occurred, and acidic groups were formed in the polymer chain. Upon repeated immersion of the sample into an acid solution, the positively charged ions of the surrounding solution were shielded by the hydrogel surface, which prevented their diffusion.

In an alkaline environment, a decrease in the degree of equilibrium swelling was observed in the second cycle and is maintained in subsequent cycles. This is because not the initial hydrogel, but the salt of the corresponding acid formed during the first cycle, undergoes repeated swelling. As a result, the sodium ions located in the environment of the hydrogel repulse similarly charged ions of the solution [51]. The cyclic character of the swelling-drying processes is illustrated in Figure 7.

2025, Vol. 2, Article ID. 2025.0014
https://doi.org/10.69709/BIOMATC.2025.108000

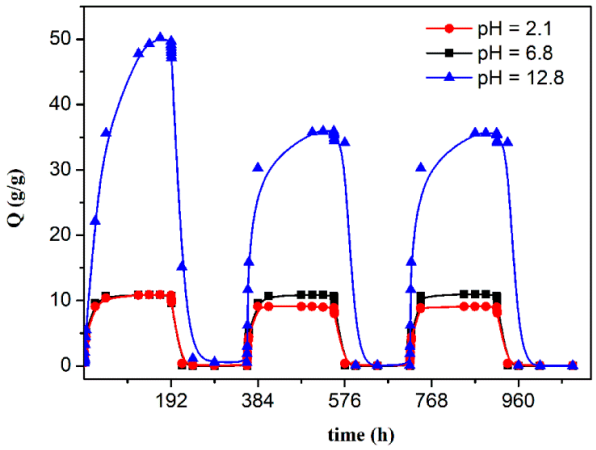


Figure 7: Cycles of the swelling-drying process of the chitosan/PAA hydrogel.

The values of Q_e depending on the pH of the swelling medium are presented in Table 1.

Table 1: The equilibrium degree of swelling in media of different pH.

pH	Q_1, g/g	Q_2, g/g	Q_3, g/g
2.1	10.9	9.1	9.0
6.8	10.8	11.0	11.0
12.8	50.2	36.0	36.0

3.4. Mechanical Properties

Mechanical properties are an important characteristic of hydrogel materials for their further use. The stress-strain curves under stretching and compression of the samples swollen to the equilibrium state in water (pH 6.8) are presented in Figure 8. Both curves are typical for the mechanical behavior of gels. The gels do not exhibit plastic deformation under either compression or tension until failure.

In order to evaluate the effect of the swelling medium on the mechanical characteristics of the gels, the samples swollen to the equilibrium state in media with pH 2.1 and 12.8 were tested. The obtained stress-strain curves were used to calculate the mechanical characteristics of the gels under compression and stretching. The values of mechanical characteristics are shown in Table 2.

As follows from Table 2, the hydrogels swollen in the alkaline medium have lower mechanical characteristics compared to those swollen in acidic and neutral media. In the alkaline solution, the gels demonstrate the highest swelling degree, i.e., the network is substantially deformed, which leads to a drop in mechanical properties.

3.5. Biological Activity

Since the prepared hydrogels are intended for use in tissue engineering, special attention should be paid to their biocompatibility and bioactivity [52]. In addition, such materials should possess a porous structure to ensure cell adhesion and proliferation.

The SEM studies revealed that these samples have a developed porous surface with micron- and submicron-sized pores (Figure 9).

The biological activity of the obtained hydrogels was estimated by the MTT test. The material was sterilized by autoclaving for 35 min at 120 °C. The samples were soaked in the DMEM nutrient medium with the addition of 1% L-glutamine, 1% antibiotics, 1% fungizone, and 10% fetal calf serum according to the standard method. Human dermal fibroblasts were seeded on the surface of the material in an amount of 30×10^3 wells. The morphology and growth pattern of the cells were recorded using light microscopy (Figure 10).

The presented images show that the morphology and wettability of the obtained hydrogels are suitable for efficient cell growth.

After the first and the fourth days of cultivation, 100 μL of MTT working solution (5 mg/mL in DPBS) was added to the samples, and they were incubated for 2 h. 1 mL of DMSO was used to dissolve formazan crystals. The resulting solution was stirred thoroughly and incubated for 5 min, then optical density measurements were performed. The data of the MTT test are presented in Figure 11.

As can be seen in the histogram, the optical density of the solution taken from the hydrogel matrices is lower than that taken from the cultural plate. Therefore, cell growth in the obtained samples is less intensive. Comparing the first and the fourth days of cultivation, the proliferation of human fibroblasts on the chitosan/PAA gels is clearly visible, which indicates the viability of cells on the studied hydrogel matrices.

3.6. Drug Release

In this work, the possibility of using the obtained chitosan/PAA systems for the controlled release of drugs from the polymer matrix was studied using a lidocaine hydrochloride (HL) solution as a model compound. The kinetics of the HL release from the chitosan/PAA hydrogel in phosphate buffer at 37 °C is shown in Figure 12. The results show that the highest drug release rate occurs in 30–40 min. This may be because the drug from the border regions of the hydrogel is released first. Then the drug release occurs by diffusion from the hydrogel volume, which results in a lower rate of the process. The

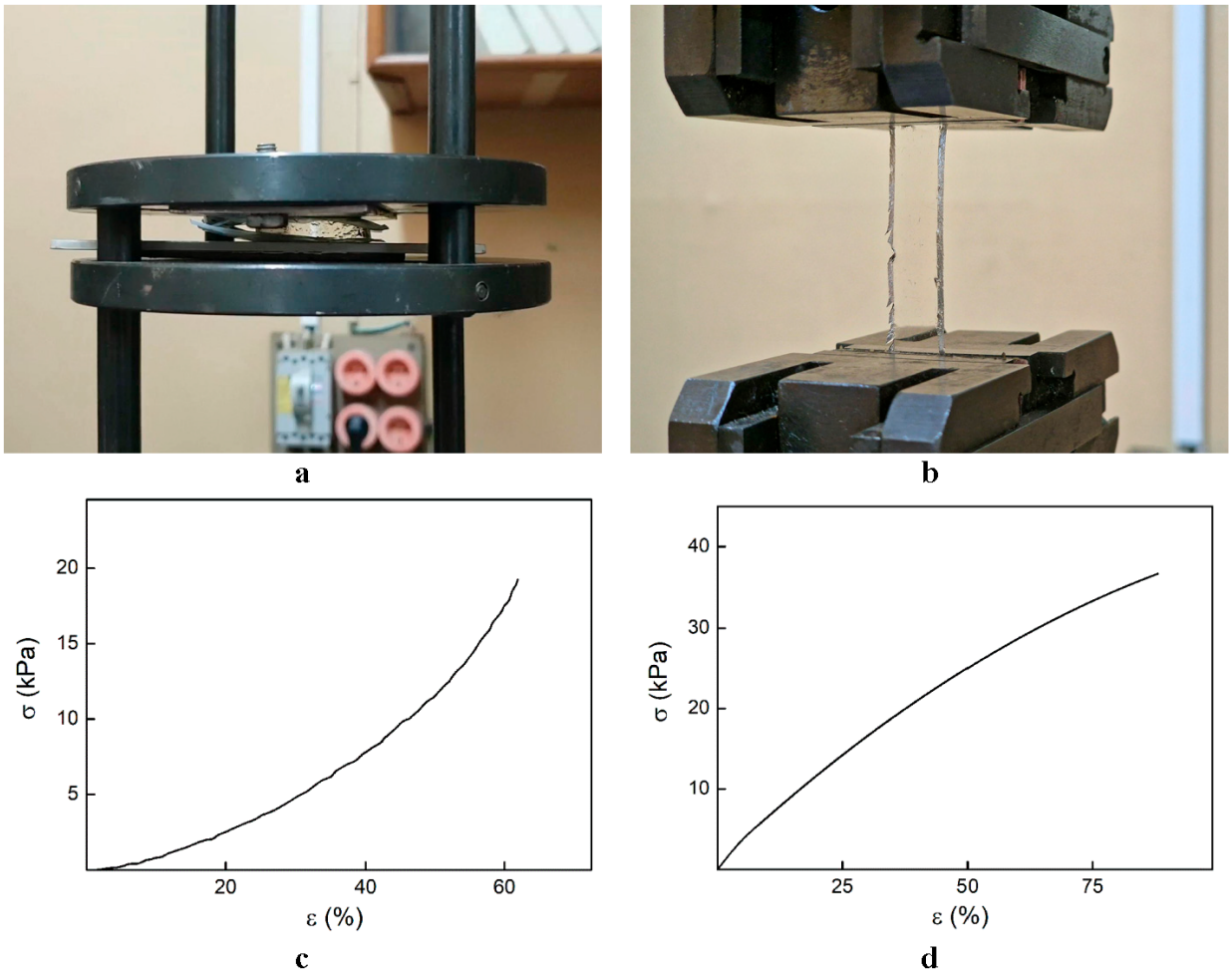


Figure 8: The picture of gels and stress-strain curves for (**a**,**c**) compression and (**b**,**d**) stretching mode.

Table 2: Mechanical characteristics of hydrogels depending on pH *.

pH	Degree of Swelling, Q, g/g	Breaking Strength, σ, kPa	Elastic Modulus, G, kPa	Deformation at Break, ε, %
2.1	10.9	23.8/41	3.35/61	68/91
6.8	10.8	19.1/37	3.31/57	62/88
12.8	50.2	5.3/11	1.82/32	46/63

* The numerator shows the characteristics for compression mode, and the denominator–stretching mode.

release of HL from the hydrogel continues for 80 h and reaches 90%. The observed prolonged release of the drug can be explained by the fact that at swelling, the dry hydrogel absorbs a significant amount of HL (up to 15 g/g), filling the entire volume of the gel.

4. Conclusions

In this work, biocompatible swelling hydrogels comprised of a natural polymer, chitosan, and a synthetic one, polyacrylamide, were obtained. The possibility of obtaining hydrogel materials of various shapes was demonstrated. The dependence of the swelling degree on the pH of the medium was studied, and the reversibility of the swelling/drying process was analyzed for chitosan/PAA systems. The conditions for achieving the minimum and maximum values of the equilibrium degree of swelling are established. It was shown that the highest values of the equilibrium degree of swelling were obtained for samples in an alkaline medium. Besides, the pH of the media affects the mechanical characteristics of synthesized hydrogels.

2025, Vol. 2, Article ID. 2025.0014
https://doi.org/10.69709/BIOMATC.2025.108000

Thus, gels swollen in an alkaline medium exhibit lower mechanical strength than those swollen in acidic and neutral media due to their higher degree of swelling in alkaline solutions. However, it should be noted that the hydrogels retain mechanical stability and elasticity in all the media studied. The biocompatibility of the obtained hydrogels was confirmed by the MTT test. Using the HL as a model compound, it was shown that synthesized hydrogels can be considered effective matrices for prolonged drug release.

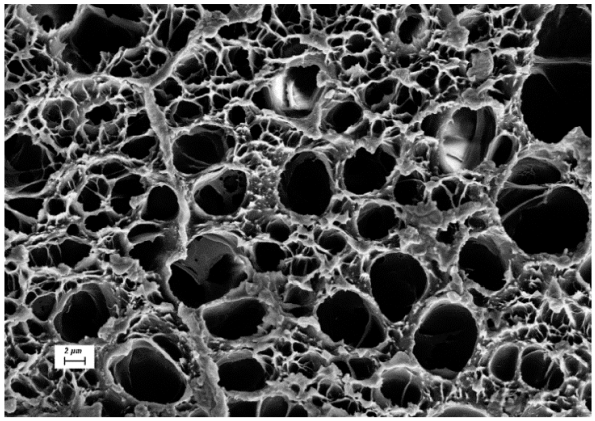


Figure 9: SEM micrographs of the chitosan/PAA hydrogel surface.

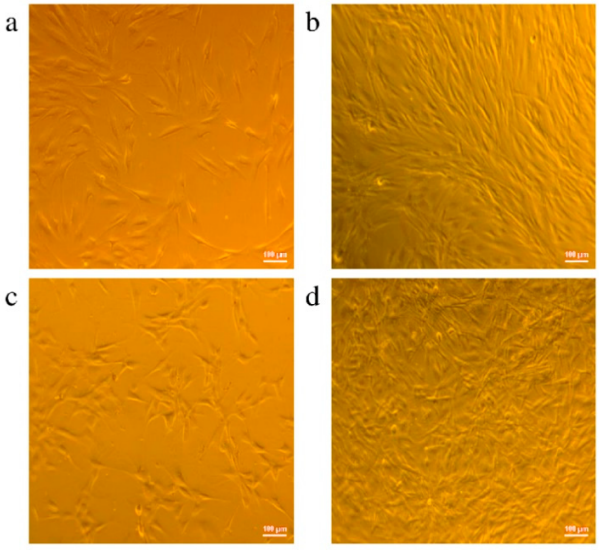


Figure 10: (**a**,**b**) Images of human dermal fibroblasts grown on the surface of culture plate and (**c**,**d**) chitosan/PAA hydrogel matrices after (**a**,**c**) 1 and (**b**,**d**) 4 days of cultivation.

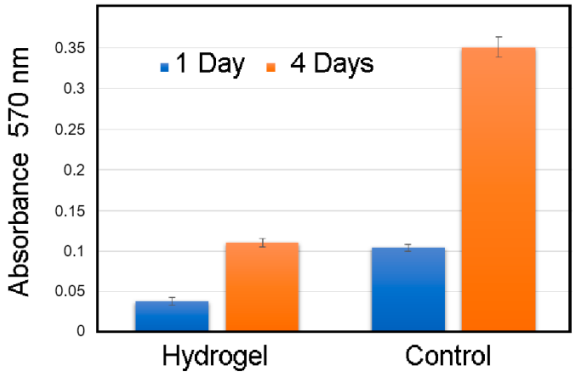


Figure 11: Viability and proliferation of human dermal fibroblasts on surfaces of hydrogels and cultural polystyrene surface (control) as determined by MTT assay. MTT test involved human dermal fibroblasts cultured on control and on the surface of the chitosan/PAA hydrogel matrices for 1 and 4 days. Optical density correlates with the number of viable cells. * $p < 0.05$.

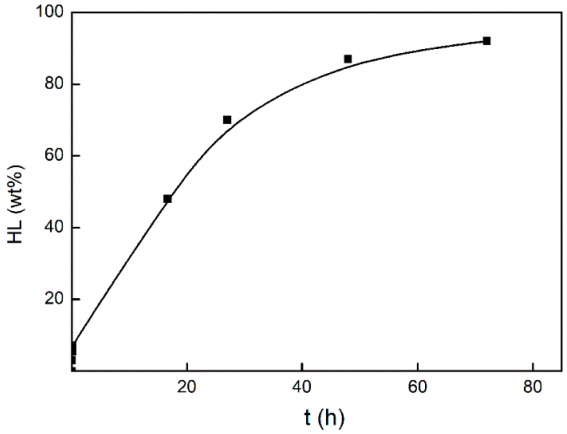


Figure 12: Amounts of HL released from chitosan/PAA hydrogels into the physiological solution at 37 °C.

Abbreviations

FTIR	Fourier transform Infrared Spectroscopy
PAA	Polyacrylamide
AA	Acrylamide
APS	Ammonium Peroxydisulfate
TEMED	N, N, N', N'-Tetramethylethylenediamine
MBAA	N, N'-Methylene-bis-acrylamide
ATR	Attenuated Total Reflectance
HL	Lidocaine Hydrochloride
SEM	Scanning Electron Microscopy
DMEM	Dulbecco's Modified Eagle Medium
DPBS	Dulbecco's Phosphate-Buffered Saline
DMSO	Dimethylsulfoxide

Author Contributions

Conceptualization: E.R., Z.Z. and N.S. (Natalia Smirnova); Methodology: Z.Z., E.R., E.V. (Elena Vlasova), I.K., K.K. and N.S. (Natalia Smirnova); Investigation: E.R., Z.Z., E.V. (Ekaterina Vyrezkova), E.V. (Elena Vlasova), I.K., N.S. (Natalia Smirnova), K.K. and N.S. (Natalia Saprykina); Writing—Original Draft Preparation: E.R., E.V. (Ekaterina Vyrezkova), E.V. (Elena Vlasova) and I.K.; Writing—Review & Editing: E.R., I.K. and Z.Z.; Supervision: E.R., I.K. and Z.Z.; Visualization: I.K. and Z.Z. All authors have agreed to and approved the final published version of the manuscript.

Availability of Data and Materials

The data that support the findings of this study are available from the corresponding author upon reasonable request.

Ethics Committee Approval and Consent to Participate

Ethical approval was not required, as the cell culture used in the study was obtained from the Vertebrate Cell Culture Collection of the Institute of Cytology of the Russian Academy of Sciences. The cell cultures are accompanied by identity documents (passports) and are suitable for use as models in open investigations of the biocompatibility of polymeric materials without the need for additional ethical permissions. Informed consent was obtained from the original donors at the time of cell collection by the Institute of Cytology Cell Bank in accordance with institutional guidelines.

Conflicts of Interest

The authors declare no conflicts of interest.

Funding

The work was carried out within the state assignment of Branch of Petersburg Nuclear Physics Institute Named by B.P. Konstantinov of National Research Centre «Kurchatov Institute»---Institute of Macromolecular Compounds---Grant Number: 124013000728-0.

Acknowledgments

Declared none.

AI Declaration

The authors confirm that no AI tool was used during the preparation of this manuscript.

References

[1] Ajmal, S.; Hashmi, F.A.; Imran, I. Recent Progress in Development and Applications of Biomaterials. *Mater. Today Proc.* **2022**, *62*, 385–391. [CrossRef]

[2] Aswathy, S.; Narendrakumar, U.; Manjubala, I. Commercial Hydrogels for Biomedical Applications. *Heliyon* **2020**, *6*, e03719. [CrossRef]

[3] Troy, E.; Tilbury, M.A.; Power, A.M.; Wall, J.G. Nature-Based Biomaterials and Their Application in Biomedicine. *Polymers* **2021**, *13*, 3321. [CrossRef] [PubMed]

[4] Nagpal, M.; Singh, S.K.; Mishra, D. Superporous Hybrid Hydrogels Based on Polyacrylamide and Chitosan: Characterization and In Vitro Drug Release. *Int. J. Pharm. Investig.* **2013**, *3*, 88–94. [CrossRef]

[5] Billiet, T.; Vandenhaute, M.; Schelfhout, J.; Van Vlierberghe, S.; Dubruel, P. A Review of Trends and Limitations in Hydrogel-Rapid Prototyping for Tissue Engineering. *Biomaterials* **2012**, *33*, 6020–6041. [CrossRef] [PubMed]

[6] Chai, Q.; Jiao, Y.; Yu, X. Hydrogels for Biomedical Applications: Their Characteristics and the Mechanisms behind Them. *Gels* **2017**, *3*, 6. [CrossRef] [PubMed]

[7] Ahmed, E.M. Hydrogel: Preparation, Characterization, and Applications: A Review. *J. Adv. Res.* **2015**, *6*, 105–121. [CrossRef]

[8] Beheshtizadeh, N.; Lotfibakhshaiesh, N.; Pazhouhnia, Z.; Hoseinpour, M.; Nafari, M. A Review of 3D Bio-Printing for Bone and Skin Tissue Engineering: A Commercial Approach. *J. Mater. Sci.* **2020**, *55*, 3729–3749. [CrossRef]

[9] Fang, W.; Yang, M.; Wang, L.; Li, W.; Liu, M.; Jin, Y.; Wang, Y.; Yang, R.; Wang, Y.; Zhang, K.; et al. Hydrogels for 3D Bioprinting in Tissue Engineering and Regenerative Medicine: Current Progress and Challenges. *Int. J. Bioprinting* **2023**, *9*, 759. [CrossRef]

[10] Hoffman, A.S. Hydrogels for Biomedical Applications. *Adv. Drug Deliv. Rev.* **2002**, *54*, 3–12. [CrossRef]

[11] Liang, J.; Dijkstra, P.J.; Poot, A.A.; Grijpma, D.W. Hybrid Hydrogels Based on Methacrylate-Functionalized Gelatin (GelMA) and Synthetic Polymers. *Biomed. Mater. Devices* **2023**, *1*, 191–201. [CrossRef]

[12] Li, H.-X.; Zhao, K.-C.; Jiang, J.-J.; Zhu, Q.-S. Research Progress on Black Phosphorus Hybrids Hydrogel Platforms for Biomedical Applications. *J. Biol. Eng.* **2023**, *17*, 8. [CrossRef]

[13] Feng, Q.; Zhang, K.; Yang, B.; Yu, Y. Editorial: Biomedical Applications of Natural Polymers. *Front. Bioeng. Biotechnol.* **2022**, *10*, 1077823. [CrossRef]

[14] Zarif, M.-E. A Review of Chitosan-, Alginate-, and Gelatin-Based Biocomposites for Bone Tissue Engineering. *Biomater. Tissue Eng. Bull.* **2018**, *5*, 97–109. [CrossRef]

[15] Mochalova, A.E.; Smirnova, L.A. State of the Art in the Targeted Modification of Chitosan. *Polym. Sci. Ser. B* **2018**, *60*, 131–161. [CrossRef]

[16] Dutta, S.D.; Patel, D.K.; Lim, K.-T. Functional Cellulose-Based Hydrogels as Extracellular Matrices for Tissue Engineering. *J. Biol. Eng.* **2019**, *13*, 55. [CrossRef] [PubMed]

[17] Pellá, M.C.; Lima-Tenório, M.K.; Tenório-Neto, E.T.; Guilherme, M.R.; Muniz, E.C.; Rubira, A.F. Chitosan-Based Hydrogels: From Preparation to Biomedical Applications. *Carbohydr. Polym.* **2018**, *196*, 233–245. [CrossRef] [PubMed]

[18] Azmana, M.; Mahmood, S.; Hilles, A.R.; Rahman, A.; Arifn, M.A.; Ahmed, S. A Review on Chitosan and Chitosan-Based Bionanocomposites: Promising Material for Combatting Global Issues and Its Applications. *Int. J. Biol. Macromol.* **2021**, *185*, 832–848. [CrossRef]

[19] Aguilar, A.; Zein, N.; Harmouch, E.; Hafdi, B.; Bornert, F.; Offner, D.; Clauss, F.; Fioretti, F.; Huck, O.; Benkirane-Jessel, N.; et al. Application of Chitosan in Bone and Dental Engineering. *Molecules* **2019**, *24*, 3009. [CrossRef]

[20] Mirzaei, B.E.; Ramazani, S.A.A.; Shafiee, M.; Danaei, M. Studies on Glutaraldehyde Crosslinked Chitosan Hydrogel Properties for Drug Delivery Systems. *Int. J. Polym. Mater. Polym. Biomater.* **2013**, *62*, 605–611. [CrossRef]

[21] Pujana, M.A.; Pérez-Álvarez, L.; Iturbe, L.C.C.; Katime, I. Biodegradable Chitosan Nanogels Crosslinked with Genipin. *Carbohydr. Polym.* **2013**, *94*, 836–842. [CrossRef]

[22] Tang, G.; Tan, Z.; Zeng, W.; Wang, X.; Shi, C.; Liu, Y.; He, H.; Chen, R.; Ye, X. Recent Advances of Chitosan-Based Injectable Hydrogels for Bone and Dental Tissue Regeneration. *Front. Bioeng. Biotechnol.* **2020**, *8*, 587658. [CrossRef]

[23] Uysal, B.Ö.; Nayır, Ş.; Açba, M.; Çıtır, B.; Durmaz, S.; Koçoğlu, Ş.; Yıldız, E.; Pekcan, Ö. 2D Materials (WS2, MoS2, MoSe2) Enhanced Polyacrylamide Gels for Multifunctional Applications. *Gels* **2022**, *8*, 465. [CrossRef] [PubMed]

[24] Azizian, S.; Hadjizadeh, A.; Niknejad, H. Chitosan-Gelatin Porous Scaffold Incorporated with Chitosan Nanoparticles for Growth Factor Delivery in Tissue Engineering. *Carbohydr. Polym.* **2018**, *202*, 315–322. [CrossRef] [PubMed]

[25] Boguang, Y.; Jingwen, X. Multicomponent Hydrogels for Tissue Engineering Applications. In *Multicomponent Hydrogels Series: Biomaterials Science Series*; The Royal Society of Chemistry: Cambridge, UK, 2023; pp. 346–380. [CrossRef]

[26] Tangri, A. Polyacrylamide Based Hydrogels: Synthesis, Characterization and Applications. *Int. J. Pharm. Chem. Biol. Sci.* **2014**, *4*, 951–959. [View Online]

[27] Yang, K.; Chen, J.; Fu, Q.; Dun, X.; Yao, C. Preparation of Novel Amphoteric Polyacrylamide and Its Synergistic Retention with Cationic Polymers. *e-Polymers* **2020**, *20*, 162–170. [CrossRef]

[28] Begum, R.; Farooqi, Z.H.; Ahmed, E.; Sharif, A.; Wu, W.; Irfan, A. Fundamentals and Applications of Acrylamide Based Microgels and Their Hybrids: A Review. *RSC Adv.* **2019**, *9*, 13838–13854. [CrossRef]

[29] Mihăilescu, C.; Dumitrescu, A.; Simionescu, B.C.; Bulacovschi, V. Synthesis of Polyacrylamide-Based Hydrogels by Simultaneous Polymerization/Crosslinking. *Rev. Roum. Chim.* **2007**, *52*, 1071–1076. [View Online]

[30] Lopatin, V.V.; Askadskii, A.A.; Peregudov, A.S.; Vasil'ev, V.G. Structure and Relaxation Properties of Medical-Purposed Polyacrylamide Gels. *J. Appl. Polym. Sci.* **2005**, *96*, 1043–1058. [CrossRef]

[31] Zhang, J.; Jing, B.; Tan, G.; Fang, S.; Wang, H. Effect of Structure of Graft on the Properties of Graft Copolymers of Acrylamide and Surfactant Macromonomers Dilute Aqueous Solutions. *J. Macromol. Sci. Part B* **2015**, *54*, 253–261. [CrossRef]

[32] Ma, G.; Li, X.; Wang, X.; Liu, G.; Jiang, L.; Yang, K. Preparation, Rheological and Drag Reduction Properties of Hydrophobically Associating Polyacrylamide Polymer. *J. Dispers. Sci. Technol.* **2019**, *40*, 171–178. [CrossRef]

[33] Kesharwani, P.; Bisht, A.; Alexander, A.; Dave, V.; Sharma, S. Biomedical Applications of Hydrogels in Drug Delivery System: An Update. *J. Drug Deliv. Sci. Technol.* **2021**, *66*, 102914. [CrossRef]

[34] Shoukat, H.; Buksh, K.; Noreen, S.; Pervaiz, F.; Maqbool, I. Hydrogels as Potential Drug-Delivery Systems: Network Design and Applications. *Ther. Deliv.* **2021**, *12*, 375–396. [CrossRef] [PubMed]

[35] Mochalova, A.E.; Smirnova, L.A.; Zaitsev, S.D.; Semchikov, Y.D.; Zaitseva, I.I.; Pavlov, G.M. Hydrodynamic and Molecular Characteristics of Graft Copolymers of Chitosan with Acrylamide. *Polym. Sci. Ser. B* **2007**, *49*, 232–235. [CrossRef]

[36] Sánchez-Cid, P.; Jiménez-Rosado, M.; Romero, A.; Pérez-Puyana, V. Novel Trends in Hydrogel Development for Biomedical Applications: A Review. *Polymers* **2022**, *14*, 3023. [CrossRef]

[37] Carpa, R.; Farkas, A.; Dobrota, C.; Butiuc-Keul, A. Double-Network Chitosan-Based Hydrogels with Improved Mechanical, Conductive, Antimicrobial, and Antibiofouling Properties. *Gels* **2023**, *9*, 278. [CrossRef]

[38] Xu, X.; He, C.; Luo, F.; Wang, H.; Peng, Z. Transparent, Conductive Hydrogels with High Mechanical Strength and Toughness. *Polymers* **2021**, *13*, 2004. [CrossRef]

[39] Wu, K.Y.; Akbar, D.; Giunta, M.; Kalevar, A.; Tran, S.D. Hydrogels in Ophthalmology: Novel Strategies for Overcoming Therapeutic Challenges. *Materials* **2024**, *17*, 86. [CrossRef]

[40] Mitura, S.; Sionkowska, A.; Jaiswal, A. Special Issue: Hydrogels in Regenerative Medicine Review Article Biopolymers for Hydrogels in Cosmetics: Review. *J. Mater. Sci. Mater. Med.* **2020**, *31*, 50. [CrossRef]

[41] Ma, C.; Dou, Y.; Li, R.; Zhang, L.; Zhou, Z.; Guo, S.; Wang, R.; Tao, K.; Liu, Y.; Yang, X. Carboxymethyl Chitosan/Polyacrylamide Double Network Hydrogels Based on Hydrogen Bond Cross-Linking as Potential Wound Dressings for Skin Repair. *Int. J. Biol. Macromol.* **2024**, *280 Pt 2*, 135735. [CrossRef]

[42] Lu, B.; Han, X.; Zou, D.; Luo, X.; Liu, L.; Wang, J.; Maitz, M.F.; Yang, P.; Huang, N.; Zhao, A. Catechol-Chitosan/Polyacrylamide Hydrogel Wound Dressing for Regulating Local Inflammation. *Mater. Today Bio* **2022**, *16*, 100392. [CrossRef] [PubMed]

[43] Chamkouri, H.; Chamkouri, M. A Review of Hydrogels, Their Properties and Applications in Medicine. *Am. J. Biomed. Sci. Res.* **2021**, *11*, 485–493. [CrossRef]

[44] Ward, I.M. *Mechanical Properties of Solid Polymers*, 3rd ed.; Wiley: Hoboken, NJ, USA, 2012. Available online: https://www.wiley.com/en-us/Mechanical+Properties+of+Solid+Polymers%2C+3rd+Edition-p-9781119967125.

[45] Brugnerotto, J.; Lizardi, J.; Goycoolea, F.; Argüelles-Monal, W.; Desbrières, J.; Rinaudo, M. An Infrared Investigation in Relation with Chitin and Chitosan Characterization. *Polymer* **2001**, *42*, 3569–3580. [CrossRef]

[46] Gaabour, L. Spectroscopic and Thermal Analysis of Polyacrylamide/Chitosan (PAM/CS) Blend Loaded by Gold Nanoparticles. *Results Phys.* **2017**, *7*, 2153–2158. [CrossRef]

[47] Van de Velde, K.; Kiekens, P. Structure Analysis and Degree of Substitution of Chitin, Chitosan and Dibutyrylchitin by FT-IR Spectroscopy and Solid State ^{13}C NMR. *Carbohydr. Polym.* **2004**, *58*, 409–416. [CrossRef]

[48] Xie, J.; Liu, X.; Liang, J.; Luo, Y. Swelling Properties of Superabsorbent Poly(acrylic acid-co-acrylamide) with Different Crosslinkers. *J. Appl. Polym. Sci.* **2009**, *112*, 602–608. [CrossRef]

[49] Huang, S.; Shen, J.; Li, N.; Ye, M. Dual pH- and Temperature-Responsive Hydrogels with Extraordinary Swelling/Deswelling Behavior and Enhanced Mechanical Performances. *J. Appl. Polym. Sci.* **2014**, *132*, 41530. [CrossRef]

[50] Zhou, Y.; Jin, L. Hydrolysis-Induced Large Swelling of Polyacrylamide Hydrogels. *Soft Matter* **2020**, *16*, 5740–5749. [CrossRef]

[51] Rohindra, D.R.; Nand, A.V.; Khurma, J.R. Swelling Properties of Chitosan Hydrogels. *South Pac. J. Nat. Appl. Sci.* **2004**, *22*, 32–35. [CrossRef]

[52] Hou, W.; Yu, X.; Li, Y.; Wei, Y.; Ren, J. Ultrafast Self-Healing, Highly Stretchable, Adhesive, and Transparent Hydrogel by Polymer Cluster Enhanced Double Networks for Both Strain Sensors and Envi-ronmental Remediation Application. *ACS Appl. Mater. Interfaces* **2022**, *14*, 57387–57398. [CrossRef]

Disclaimer/Publisher's Note: The views expressed in this article are those of the author(s) and do not necessarily reflect the views of the publisher or editors. The publisher and editors assume no responsibility for any injury or damage resulting from the use of information contained herein.